Chinese Chemical Letters 31 (2020) 2717–2720

Contents lists available at ScienceDirect

Chinese Chemical Letters

journal homepage: www.elsevier.com/locate/cclet

Communication

Hierarchical porous induced competent removal of low concentration azo dye molecules by generating a leachy crystalline structure H-MIL-53(Fe)

Tao Feng[a,b], Jean Pierre Bavumiragira[a,b], Mumbi Anne Wambui[a,b], Daniel Manaye Kabtamu[a,b], Krisztina László[c], Ying Wang[a,b,*], Fengting Li[a,b,*]

[a] State Key Laboratory of Pollution Control and Resources Reuse, College of Environmental Science and Engineering, Tongji University, Shanghai 200092, China
[b] Shanghai Institute of Pollution Control and Ecological Security, Shanghai 200092, China
[c] Department of Physical Chemistry and Materials Science, Budapest University of Technology and Economics, H-1521 Budapest, Hungary

ARTICLE INFO

Article history:
Received 14 February 2020
Received in revised form 2 April 2020
Accepted 24 April 2020
Available online 5 May 2020

Keywords:
H-MIL-53(Fe)
Salicylic acid
Leachy crystalline
Adsorption
Orange G removal

ABSTRACT

The development in technology of synthetic azo dyes, has led to excessive water resources pollution. Even at lower concentration they can impart the quality of water and human life. Herein, we have developed a novel synthesis strategy *via* introducing salicylic acid (SA) for the synthesis of a leachy crystalline material H-MIL-53(Fe) with hierarchical pores (HP) and exposed coordination unsaturated sites (CUS), which had higher surface area and larger pore volume than the as synthesized MIL-53(Fe). Due to these characteristics, H-MIL-53(Fe) was competent removal of orange G (OG, one of the frequently used azo dyes) with equilibrium in 300 min and the maximum adsorption capacity of 163.9 mg/g. The adsorption mechanism of OG onto H-MIL-53(Fe) was mostly based on electrostatic attraction between CUS of H-MIL-53(Fe) along with HP as active species to OG diffusion and bind. By comparing H-MIL-53(Fe) with other adsorbents for OG adsorption, it is undoubtedly that H-MIL-53(Fe) can be used as a promising adsorbent for OG removal from aqueous solutions.

Nowadays dyes pollution is an increasingly worldwide concern [1,2]. It is estimated that more than half of the dyes pollution are azo derivatives, making them the major class that becomes an integral part of the industrial wastewater [3,4]. Orange G (OG) is one of the azo dyes which is frequently used in the pulp and paper industries [5]. The occurrence of —N=N— chromophore group and aromatic structure make it non-biodegradable, resistant to oxidizing agent and light. Even at lower concentration equals to 1 mg/L, it can affect the quality of water and human life which causes even cancer [6]. Therefore, it is imperative to remove dyes from the aquatic environment by using low cost, easy operation and efficiency technology.

Among different technologies for removal of dye from wastewater such as flocculation, ozonation, and membrane filtration [7], adsorption is reported to be one of the most competitive methods for its efficiency, simplicity and low cost [8]. Different materials such as activated carbon [9], zeolite [10], clay [11], and molecular sieve [12] have been studied. However, the defects of traditional adsorbents are their low efficiency and difficulty in regeneration. Metal-organic frameworks (MOFs) are a new class of porous, crystalline materials possessing a large surface area, tunable pore size and shape, adjustable composition, and functional pore surface that show great promise for use in adsorption [13,14]. Among them, MIL-53(Fe) have small size and flexible structure properties leading to convenience of parting, immense reactivity and large number of active sites for interactions with contaminants which were made them to be used as promising adsorbents [15]. But it still possessed problems with adsorption dyes. For example, MIL-53(Fe) is completely closed pore structure, which greatly limits its specific surface area and hence its adsorption capacity and efficiency. Therefore, it is highly desirable to create the hierarchical pores (HP) for obtaining a large specific surface area and improving mass transfer.

Previous researchers have reported some HP creation methods, such as direct synthesis and templating methods [16–20]. However, the achievements of these approaches are limited in some respects. New linkers are difficult to synthesis and templates

* Corresponding authors at: State Key Laboratory of Pollution Control and Resources Reuse, College of Environmental Science and Engineering, Tongji University, Shanghai 200092, China.
E-mail addresses: yingwang@tongji.edu.cn (Y. Wang), fengting@tongji.edu.cn (F. Li).

https://doi.org/10.1016/j.cclet.2020.04.044

are usually randomly added to the frame during the site assembly process [21]. Thus removing them may cause collapse of the frame, although the pores formed in the MOFs, stability is worse [22,23]. Hence, the coordinated molecule, similar to the linker, which partially blocks the traditional linker assembly brings new opportunities in the synthesis process. Due to the coordination between small molecules, the coordinated molecule can produce defects in MOFs crystal and the stability of the framework can be maintained.

In this study, a novel strategy to synthesize H-MIL-53(Fe) *via* introducing the small molecule salicylic acid (SA) as the coordinated molecule is proposed, and it was selected as an adsorbent to be used in removal of OG from aqueous solution. With the coordination unsaturated sites (CUS) and HP structure, the resulting composite materials, H-MIL-53(Fe), offers new opportunities for the adsorption of OG azo dye.

The MIL-53(Fe) was synthesized by the traditional method with the firmness smooth surface (Fig. 1a). The novel strategy to H-MIL-53(Fe) synthesis was shown in Fig. 1b. Particularly, the Fe^{3+} first mixed with SA forming a purple solution at room temperature (r.t.) due to the complexation of Fe^{3+}–SA. This is a conventional color reaction, which has been applied to detecting other related aspects [24]. Then, the self-assembly process of Fe^{3+} and H_2BDC was performed under solvothermal conditions. As complex of Fe^{3+}–SA has already existed, it has a competitive coordination and a certain steric hindrance effect on the normal coordination of Fe^{3+} and H_2BDC, which disrupts the normal assembly process. Meanwhile, when H_2BDC forms stable complexes with Fe^{3+}, the interactions of Fe^{3+} with SA are unstable, therefore, they are removed from the system which results in HP and CUS (pale blue circles) during the rapid growth of crystals. The crystal defects and nanounits constitute hierarchical porosity together. The surface morphology of H-MIL-53(Fe) is seen like crystals of rough surface and is sorted in irregular octahedral shape according to the scanning electron microscope (SEM) image. The hierarchical porosity was further confirmed by transmission electron microscopy (TEM) images. The TEM image depicted that defects are on the surface of H-MIL-53 (Fe), while it exhibits novel leachy crystalline structure.

To further explain the porosity of H-MIL-53(Fe), N_2 adsorption-desorption measurements were performed. it was observed to have the BET surface area of 187.85 m^2/g, which is 20 times more than MIL-53(Fe) (Fig. 2a) [25]. The significant increase on the surface area of H-MIL-53(Fe) can be explained by the fact that the salicylic acid (SA) used during its synthesis has contributed to the increase of more opened pores distributed in H-MIL-53(Fe) (Table S1 in Supporting information). Moreover, the HP of H-MIL-53(Fe) can be created through SA addition. With the presence of SA, the pores sizes show the micropore and mesoporous distribution consistent with HRTEM results (Fig. 2b). Moreover, powder X-ray diffraction (XRD) patterns shows the crystal structure of the synthesized materials H-MIL-53(Fe) and MIL-53 (Fe) with the main diffraction peaks found to some extent, although peak intensity reduces slightly (Fig. 2c). It can be explained that H-MIL-53(Fe) maintained a fine crystalline structure well commensurate with previous reports for MIL-53(Fe) [26]. Guided by the weight loss information on MIL-53(Fe) from thermogravimetric analyzer (TGA) curves, it showed a sharp step at around 492 °C and the similar curve of H-MIL-53(Fe) possessed almost the same step in the 491 °C (Fig. 2d). This indicates that adding SA can create leachy crystalline structure without further affecting the stability. Meanwhile, according to Fourier transform infrared spectroscopy (FTIR) spectrums (Fig. S1 in Supporting information), the change of absorption peak at 1528 cm^{-1} and there is a slight loss of carboxylate groups (1434 cm^{-1}) [27] indicating that SA has affected the coordination between linker (H_2BDC) and irons while the stability of the framework can be maintained.

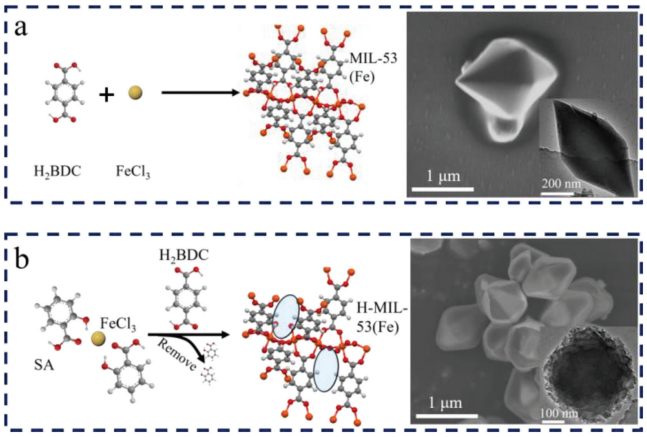

Fig. 1. Schematic diagram of reactions process in synthesis and SEM, TEM images of MIL-53(Fe) (a); and H-MIL-53(Fe) (b).

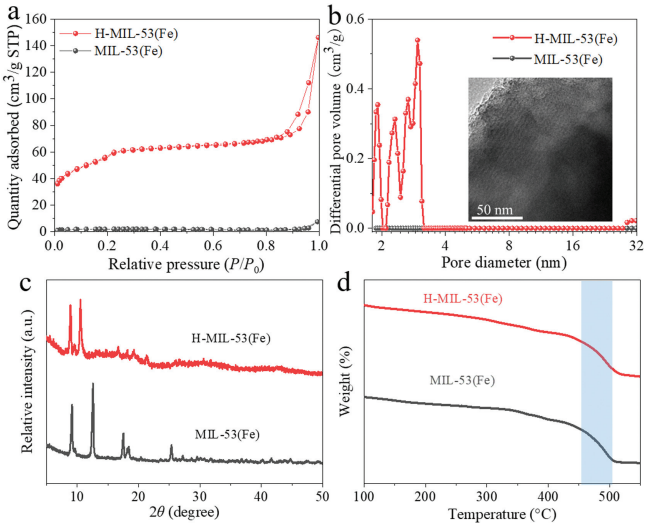

Fig. 2. N_2 adsorption-desorption isotherms (a); pore size distributions using density functional theory (DFT) method (insert: HRTEM of H-MIL-53(Fe)) (b); XRD patterns (c); and TGA (d) of H-MIL-53(Fe) and MIL-53(Fe).

Leachy crystalline structures are designed to help improve mass transfer efficiency and obtain more CUS active sites. To test performance of the novel adsorbents, we determine the equilibrium time of adsorption of OG on H-MIL-53(Fe) and MIL-53(Fe). It was found that the removal rate of the dye continuously increases and then remained constant after 300 min. Therefore, a period of 300 min was selected for further experiments. Fig. 3a shows that there was a dramatic increase of OG removal in the first 60 min for both adsorbents and was slow till 300 min. This can be explained that there were more vacant surface sites for adsorption on the H-MIL-53(Fe) than MIL-53(Fe) due to the relative high surface areas and the specific defects. However, with the increase of time, the surface adsorption sites tend to be saturated, and only the specific leachy crystalline structure of H-MIL-53(Fe) can enable the reaction to proceed further [28]. The effect of initial OG concentration on adsorption of H-MIL-53(Fe) and MIL-53(Fe) was investigated at different concentrations (20–100 mg/L) by keeping other parameter constant (adsorbent dose of 0.02 g, pH 4, 300 min, at 298 K) (Fig. 3b). It was found that the adsorption capacity increased and gradually reached a plateau when increasing the initial OG concentrations. However, when the

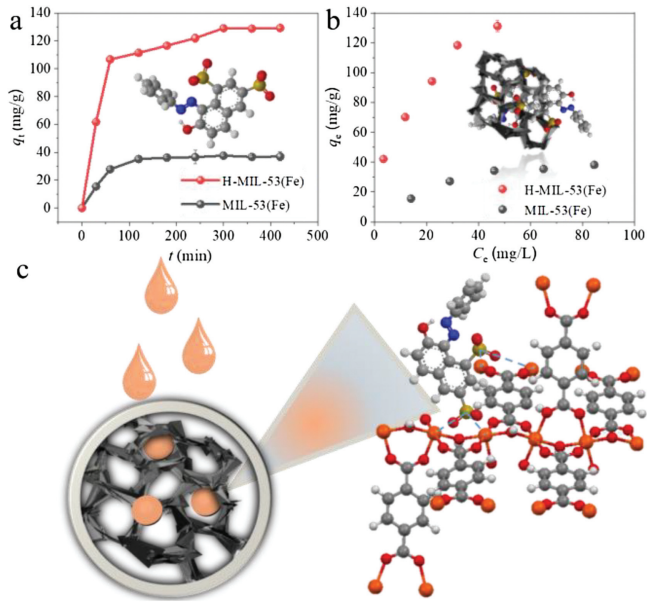

Fig. 3. Comparison of adsorption efficiency and adsorption capacity between H-MIL-53(Fe) and MIL-53(Fe): Effect of contact time on the adsorption capacity with 100 mg/L OG (insert: the structure of OG) (a), and effect of the initial concentration of OG on the adsorption capacity for 300 min (insert: the diagram of OG adsorption) (b). Schematic illustration of the adsorption mechanism of OG (c).

initial OG concentration was 50 mg/L, MIL-53(Fe) basically reached the adsorption equilibrium. Even if the initial OG concentration reached 100 mg/L, H-MIL-53(Fe) still not reach equilibrium, indicating that H-MIL-53(Fe) had a larger adsorption capacity than MIL-53(Fe) [29]. This was because that there were more sufficient binding sites available of H-MIL-53(Fe) for OG adsorption which resulted in a better interaction between dye molecules and adsorbent. After comparing the performance of H-MIL-53(Fe) with other adsorbents (Table S2 in Supporting information), it can be concluded that a novel leachy crystalline H-MIL-53(Fe) was synthesized, in a facile efficient and low cost strategy, suggesting a promising adsorbent in the removal of OG azo dye from aqueous solutions.

The initial pH plays an important role in adsorption process and is a major parameter that controls the adsorption properties of a material. It affects the charge distribution of the surface of the adsorbents as well as OG molecules. As shown in Fig. S2 (Supporting information), from pH 3 the adsorption capacity increases dramatically and attains the maximum at pH 4 for both adsorbents. The decrease observed from pH 5–10 may be explained by the conversion of OG molecules to OG^+ which resulted in a repulsion characteristic over the positively charged surface of both H-MIL-53(Fe) and MIL-53(Fe) [30]. However, H-MIL-53(Fe) showed continual removal of OG at pH range 6–8 due to more active sites than those of MIL-53(Fe) and its surface became less negatively charged. Therefore H-MIL-53(Fe) showed a higher OG removal in a wide pH range than MIL-53(Fe). The adsorbed amount of OG increased with increasing adsorbent amount. Therefore, this can be described that the more increase in the adsorbent dose, the more active sites will also be available for OG dye molecules [31]. Beyond 0.02 g of H-MIL-53(Fe), the adsorption efficiency is greatly reduced for initial concentration of 20 mg/L OG (Fig. S3 in Supporting information). Therefore 0.02 g was selected to be used for the all experimental batches. Moreover, the adsorption capacity of OG was still higher than 127 mg/g in three successive cycles, showing an excellent capacity for regeneration (Fig. S4 in Supporting information). The small decrease in adsorption performance may result from a minor decrease in crystallinity of the used MOF, however, the mainly diffraction peaks remained basically unchanged after reaction for three cycles (Fig. S5 in Supporting information)

After adsorption, the peak was enhanced at position 1507 cm^{-1} —N=N— bending) due to the overlap of the new peak with the original one and the new band 1044 cm^{-1} (*vs.* ($-SO_3$) stretching) [32] was obviously presented in the spectrum of H-MIL-53(Fe)-OG (Fig. S6 in Supporting information). These peaks were present due to the characteristic adsorption peaks of OG, which suggested that OG was successfully adsorbed on H-MIL-53(Fe). Coupled with the results of the pH study, mechanism is mainly based on the electrostatic attraction between Fe–$(OH)_x^+$ cations and the negatively charged sulfonic group of OG–SO_3^- [33] (Fig. 3c). A new synthetic strategy gives H-MIL-53(Fe) leachy crystalline structure with HP and more CUS active sites. Because of these unique characteristics: 1) H-MIL-53(Fe) provides relatively high specific surface area which provides sufficient space to host the adsorption active sites; 2) HP is another key point we should pay attention to, since it effected the OG diffusion inside the framework once the pollutants adsorbed on the surface. OG can be easily coordinated with the metal cations in the MOF, and consequently the adsorption capacity increase; 3) CUS fabricated through the strategy provides a novel approach for MOF materials, and the generation of CUS is another factor which will have great effects on dyes removal. Hence, OG–SO_3^- is more easily diffused and binded with H-MIL-53(Fe). This electrostatic attraction well explains why the adsorption capacity of H-MIL-53(Fe) is 3 times higher than that of MIL-53(Fe).

To investigate the adsorption kinetics and to explain the sorption mechanism of OG to H-MIL-53(Fe) and MIL-53(Fe), *pseudo*-first-order (Fig. 4a) and *pseudo*-second-order (Fig. 4b) kinetics models were applied to fit the experimental data. As the correlation coefficients of the *pseudo*-second-order rate model for the linear relation of *t versus t*/*qt* was very close to 1, it confirmed that OG had been adsorbed *via* chemical reactions [34]. And also, the relevant parameters and normalized standard deviation are given in Table S3 (Supporting information).

The adsorption isotherms of OG on H-MIL-53(Fe) and MIL-53 (Fe) were present. And the fitting results based on the Langmuir and Freundlich models were shown in Figs. 4c and d. High

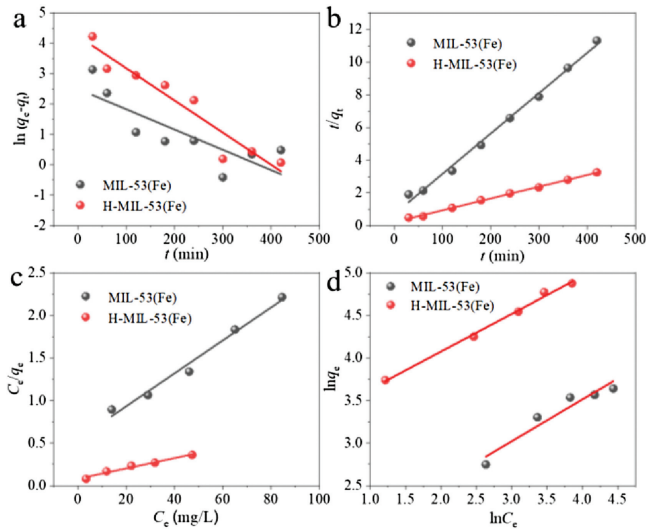

Fig. 4. Adsorption kinetic fitting with (a) *pseudo*-first-order model and (b) *pseudo*-second-order model on H-MIL-53(Fe) and MIL-53(Fe) with 100 mg/L OG at 298 K. Adsorption data simulation with (c) Langmuir and (d) Freundlich isotherm adsorption models on H-MIL-53(Fe) and MIL-53(Fe) with 20-100 mg/L OG for 5 h at 298 K.

correlation coefficients (R^2) suggested that the experimental data of MIL-53(Fe) fitted to the Langmuir model well and interestingly Langmuir and Freundlich isotherm both shows great description of H-MIL-53(Fe). Based on the hypothesis condition of Langmuir model, it was speculated that the former adsorbent underwent monolayer chemisorption of OG onto their surface. However, it is more appropriate to interpret that monolayer and multilayer adsorption processes both occur on the heterogeneous H-MIL-53 (Fe). The theoretical maximum adsorption capacity (q_{max}) obtained from Langmuir model was calculated to be 163.9 mg/g, which was higher than that of MIL-53(Fe). The relevant parameters and normalized standard deviation are also given in Table S4 (Supporting information).

In summary, H-MIL-53(Fe) have been developed *via* an easy method and used for OG removal. SA, a defect-generation molecule, was introduced to fabricate a hierarchically porous crystalline structure with CUS active adsorption sites which guarantee the equilibrium time in 300 min and the maximum adsorption capacity of 163.9 mg/g. The adsorption of OG on H-MIL-53(Fe), was mostly based on electrostatic attraction along with the monolayer and multilayer adsorption processes both occurring on the heterogeneous H-MIL-53(Fe). In addition, H-MIL-53(Fe) was applied for the removal of OG in surface water, despite of various ions and organics interference, the removal efficiency still high (Fig. S7 in Supporting information). These merits of high adsorption performance make the prepared H-MIL-53(Fe) particularly desirable for efficient OG removal in industrial application.

Declaration of competing interest

The authors declare that they have no known competing financial interests or personal relationships that could have appeared to influence the work reported in this paper.

Acknowledgments

This work was supported by the National Natural Science Foundation of China (Nos. 21876132, 21577100), the National Program for Support of Top-Notch Young Professionals, Shanghai Rising-Star Program (No. 18QA1404300), the Fundamental Research Funds for the Central Universities (Nos. 22120180102, 22120200146), and Young Excellent Talents in Tongji University (No. 2015KJ001), Science & Technology Commission of Shanghai Municipality (No. 18DZ1204400).

Appendix A. Supplementary data

Supplementary material related to this article can be found, in the online version, at doi:https://doi.org/10.1016/j.cclet.2020.04.044.

References

[1] R. Rakhshaee, M. Giahi, A. Pourahmad, Chin. Chem. Lett. 22 (2011) 501–504.
[2] B. Xu, H. Zheng, H. Zhou, et al., J. Mol. Liq. 256 (2018) 424–432.
[3] Y.N. Patel, M.P. Patel, Chin. Chem. Lett. 24 (2013) 1005–1007.
[4] A. El-Ghenymy, F. Centellas, J.A. Garrido, et al., Electrochim. Acta 130 (2014) 568–576.
[5] J. Sun, L. Qiao, S. Sun, G. Wang, J. Hazard. Mater. 155 (2008) 312–319.
[6] P.A. Carneiro, G.A. Umbuzeiro, D.P. Oliveira, M.V. Zanoni, J. Hazard. Mater. 174 (2010) 694–699.
[7] M.A.M. Salleh, D.K. Mahmoud, W.A.W.A. Karim, A. Idris, Desalination 280 (2011) 1–13.
[8] M. Arulkumar, P. Sathishkumar, T. Palvannan, J. Hazard. Mater. 186 (2011) 827–834.
[9] V. Gomez, M.S. Larrechi, M.P. Callao, Chemosphere 69 (2007) 1151–1158.
[10] S. Wang, Z.H. Zhu, J. Hazard. Mater. 136 (2006) 946–952.
[11] S.S. Tahir, N. Rauf, Chemosphere 63 (2006) 1842–1848.
[12] Q. Qin, J. Ma, K. Liu, J. Hazard. Mater. 162 (2009) 133–139.
[13] T.M. McDonald, W.R. Lee, et al., J. Am. Chem. Soc. 134 (2012) 7056–7065.
[14] Y. Wang, Y. Zhu, A. Binyam, et al., Biosens. Bioelectron. 86 (2016) 432–438.
[15] P. Horcajada, C. Serre, G. Maurin, et al., J. Am. Chem. Soc. 130 (2008) 6774–6780.
[16] D. Feng, T.F. Liu, J. Su, et al., Nat. Commun. 6 (2015) 5979–5986.
[17] C.C. Liang, Z.L. Shi, C.T. He, et al., J. Am. Chem. Soc. 139 (2017) 13300–13303.
[18] W. Zhang, Y. Liu, G. Lu, et al., Adv. Mater. 27 (2015) 2923–2929.
[19] H. Yu, D. Xu, Q. Xu, Chem. Commun. 51 (2015) 13197–13200.
[20] Y.N. Wu, M. Zhou, B. Zhang, et al., Nanoscale 6 (2014) 1105–1112.
[21] L.B. Sun, J.R. Li, J. Park, H.C. Zhou, J. Am. Chem. Soc. 134 (2011) 126–129.
[22] R.E. Morris, J. Čejka, Nat. Chem. 7 (2015) 381–388.
[23] P.S. Wheatley, P. Chlubná-Eliášová, H. Greer, et al., Angew. Chem. Int. Ed. 53 (2014) 13210–13214.
[24] I. Bezverkhyy, E. Popova, N. Geoffroy, F. Herbst, J.P. Bellat, J. Mater. Chem. A 4 (2016) 8141–8148.
[25] R. El Osta, A. Carlin-Sinclair, N. Guillou, et al., Chem. Mater. 24 (2012) 2781–2791.
[26] L. Feng, S. Yuan, L.L. Zhang, et al., J. Am. Chem. Soc. 140 (2018) 2363–2372.
[27] K. Cha, K. Park, Talanta 46 (1998) 1567–1571.
[28] Z. Hasan, J. Jeon, S.H. Jhung, J. Hazard. Mater. 209-210 (2012) 151–157.
[29] T. Feng, J. Xu, C. Yu, et al., J. Hazard. Mater. 367 (2019) 26–34.
[30] C. Chen, M. Zhang, Q. Guan, W. Li, Chem. Eng. J. 183 (2012) 60–67.
[31] E. Yılmaz, E. Sert, F.S. Atalay, J. Taiwan Inst. Chem. Eng. 65 (2016) 323–330.
[32] C. Bauer, P. Jacques, A. Kalt, Chem. Phys. Lett. 307 (1999) 397–406.
[33] C. Ling, Y. Zhao, Z. Ren, et al., Chin. Chem. Lett. 30 (2019) 2196–2200.
[34] D. Chen, Y. Li, J. Zhang, et al., J. Hazard. Mater. 243 (2012) 152–160.